Nuclear Level Densities

Stéphane Hilaire[1,2,*], *Stéphane* Goriely[3], and *Sophie* Péru[1,2]

[1]CEA, DAM, DIF, F-91297 Arpajon, France
[2]Université Paris-Saclay, CEA, LMCE, 91680 Bruyères-le-Châtel, France
[3]Institut d'Astronomie et d'Astrophysique, Université Libre de Bruxelles, Campus de la Plaine CP 226, 1050 Brussels, Belgium

Abstract. Nuclear reaction models, and in particular compound nucleus reactions, require the knowledge of nuclear level densities (NLDs), among other ingredients. For decades, analytical expressions have been used in nuclear reaction codes, due to the freedom they offer to the user to modify their associated parameters in order to fit cross sections. The development of computational resources has opened a new era, roughly 20 years ago, by allowing calculation of NLDs from more microscopic approaches and their use in reaction codes through tables stored in databases. During this 20 year period, several approaches have been developed to improve step by step the physical description of NLDs. We review some of these efforts and show where we are now and what we foresee as future improvements.

1 Introduction

The modelling of nuclear reactions relies on several physical ingredients which, in turn, require various input data. Among them, the nuclear level density (NLD) is of particular importance as soon as the decay from a nucleus occurs towards a channel located in the continnuum of the residual nucleus formed. The continuum of a nucleus is defined above an arbitrary excitation energy corresponding to the energy above which one considers the low energy discrete level scheme to be incomplete. This occurs generally at an excitation enegy above 1-2 MeV except for very light nuclei for which discrete levels can be resolved up to higher energies. When considering particle-induced nuclear reactions on heavy enough target, the compound nucleus is formed at least at the projectile separation energy, therefore generally in the continuum. As a consequence, even for low incident particle energy, the nuclear reaction description will at least require the use of the compound level density to describe the gamma decay. With increasing incident projectile energy, inelastic reaction channel will also open and level density for the target and residual nuclei will also come into play above a given threshold. Last but not least, as we will see later, the fission process also requires the use of nuclear level densities.

Nuclear level densities have been the subject of many publications [1] since the pioneering work of Bethe [2] which provided the first analytical expression. These empirical formulae (which will be briefly described together with the main data on which one can adjust them in Section 2) are often used to fit experimental cross sections, due to their simplicity and the free parameters they contain which offer a great flexibility. However, they are based on rather crude approximations which do not account for subtle non-statistical effects and since they rely on adjustable parameters, they are questionable as soon as one has to deal with nuclei located away from the valley of stability where data are unavailable to perform the adjustment. To improve the predictions, a lot of efforts have thus been devoted to obtain NLDs from microscopic approaches based on sound physical bases. These will be reviewed in Section 3 together with an emphasis on their strengths and weaknesses. We will finally show in Sec. 4 the promising features of a recent approach before drawing conclusions and prospects for the coming years.

*e-mail: stephane.hilaire@cea.fr

2 Basic features on level densities

As mentioned in the introduction, if one can observe individual levels in a nucleus at low excitation energy, their spacing decreases with increasing energy so that at some point they cannot be resolved and therefore distinguished anymore. Plotting the cumulated number of levels as function of energy provides the evidence that this number increases exponentially with increasing excitation energy U, so that the NLD can be described at low energy by the so-called constant temperature law [3]

$$\rho(U) = \frac{1}{T}\exp\left[\frac{E-E_0}{T}\right]. \quad (1)$$

This exponential increase is also confirmed theoretically for higher energies within the framework of the Fermi Gas model which enables to obtain an empirical expression for the spin- and parity-dependent level density which reads

$$\rho(U,J,\pi) = \frac{1}{2}\times\frac{\sqrt{\pi}}{12}\frac{\exp\left(2\sqrt{aU}\right)}{a^{1/4}U^{5/4}}\times\frac{2J+1}{2\sqrt{2\pi}\sigma^3}\exp\left[-\frac{(J+1/2)^2}{2\sigma^2}\right] \quad (2)$$

where the so-called spin cut-off factor σ turns out to be proportional to the nuclear temperature $T = \sqrt{U/a}$ (i.e. $\sigma^2 = \mathcal{K}\ T$). Eq. 1 is often used for low excitation energies and connected with Eq. 2 above a given matching energy (determined to ensure the continuity of the NLD and of its derivative) to provide the so-called composite NLD formula.

A useful source of information to test the NLD model and calibrate them is the so-called s-wave mean spacing D_0 which corresponds to the spacing of the resonances observed in the total absorption cross section measured within a energy range of a few tens of eV when a thermal neutron impinges a target nucleus of spin I_t and parity π_t. In this case, one has $1/D_0 = \rho(B_n, 1/2, \pi_t)$ for an even-even target and $1/D_0 = \rho(B_n, I_t{+}1/2, \pi_t){+}\rho(B_n, I_t{-}1/2, \pi_t)$ otherwise. Assuming the $\mathcal{K}$ factor of the spin cut-off parameter is the rigid body value of the nucleus moment of inertia, it is straightforward to adjust the level density parameter a in Eq.2. The results are plotted in Fig. 1(a) in which a shift is observed depending upon whether the nucleus is even-even, odd-even or odd-odd. This shift reflects the fact that the D_0 values are lower for odd-odd nuclei than for odd-A nuclei which in turn is lower than for even-even ones because of pairing correlations. Such a dispersion disappears if one simply replaces in Eq. 2 U by $U-\Delta$ where $\Delta = 0$ for odd-odd nuclei, $12/\sqrt{(A)}$ for odd-A nuclei and $24/\sqrt{(A)}$ for even-even ones (Fig. 1(b). In this case, the level density parameter roughly behaves like $A/8$ except in the vicinity to magic numbers where shell effects are still observed. A way to account for shell effects consists in introducing a shell correction in the level density parameter using, for example, the so-called Ignatyuk formula which enables to obtain an almost smooth level density parameter behaviour as function of the mass number A. The $A/8$ level density behaviour differs from the Fermi Gas prediction ($A/13$). This is interpreted as a consequence of the fact that nuclei exhibit collective vibrational and rotational levels which are not accounted for properly within the framework of the Fermi Gas model. If such collective effects are explicitly treated introducing collective enhancement factors in the level density expression, the level density parameter is shown to be reduced to the expected dependence of $A/13$.

Such collective effects are particularly important when dealing with fission. Indeed, in order to determine fission cross sections, level densities on top of the fission barriers are required. The latter are supposed to describe transition states through which the fission process occurs. In this case, since no experimental data are available, the fission level densities are adjusted to fit fission cross sections. Feedback from such type of analysis have shown that the rotational enhancement had to be accounted for and depends on the broken symmetries of the nucleus along the fission path. Several expressions can be considered [1, 4] : generally speaking, the more symmetries are broken, the higher the enhancement.

3 Traditional microscopic approaches

As mentioned above, due to the lack of experimental data and the crude approximations on which analytical expressions are based, efforts have been conducted to provide level densities based on microscopic approaches. Two types of approaches can be distinguished : The local and systematic ones.

3.1 Local approaches

Local approaches aim at being the most exact but they are for now limited either to low mass nuclei or to specific mass regions. Shell model and Moments approaches [5, 6] as well as Shell-model Monte Carlo [7–10] approaches belong to this family. The interaction on which they rely is usually adjusted on experimental data and also restricted to local mass regions. On top of that, these approaches require too much computing power to be used extensively. Yet, they account for many-body effects in a coherent way and treat consistently in one unique framework both the individual and collective nuclear properties. Fig. 2 shows a typical illustration of what Shell-model Monte Carlo calculations yield for the collective enhancement factor in three Nd isotopes [12]. One can note that the enhancement is significantly different for a spherical (^{146}Nd) and a deformed (^{150}Nd) nucleus and that it displays structure clearly different from what the usual analytical expressions use.

These methods also provide spin- and parity-dependent results at the price of an extra numerical cost for Shell-model Monte Carlo. An example is illustrated in Fig. 3 for ^{58}Ni where one can clearly observe non-statistical features for low energies as well as a clear parity non-equipartition.

3.2 Global approaches

Global approaches are more approximate but can be used over the whole periodic table without any particular difficulty. The price to pay is the separation between collective and non-collective levels. In practice, incoherent level densities are estimated from particle-hole excitations and collective effects are added on top of them. The first systematic method providing NLD tables for all nuclei has been obtained in 2001 [14]. Incoherent NLDs were obtained using the saddle point approximation with nuclear structure properties (single-particle level, pairing, deformation) deduced from Hartree-Fock-BCS (HF+BCS) predictions based on a Skyrme interaction, and, for deformed nuclei, rotational bands were explicitly constructed. A damping of deformation with increasing energy was also introduced. Although this mean-field statistical method does not go beyond the statistical spin distribution and parity equipartition assumptions, it provides a rather good description of s-waves mean spacings (see middle panel of Fig. 4).

To remove the aforementioned limitations, the combinatorial approach has been proposed. It was initially applied globally using the BSk13 Skyrme interaction [15]

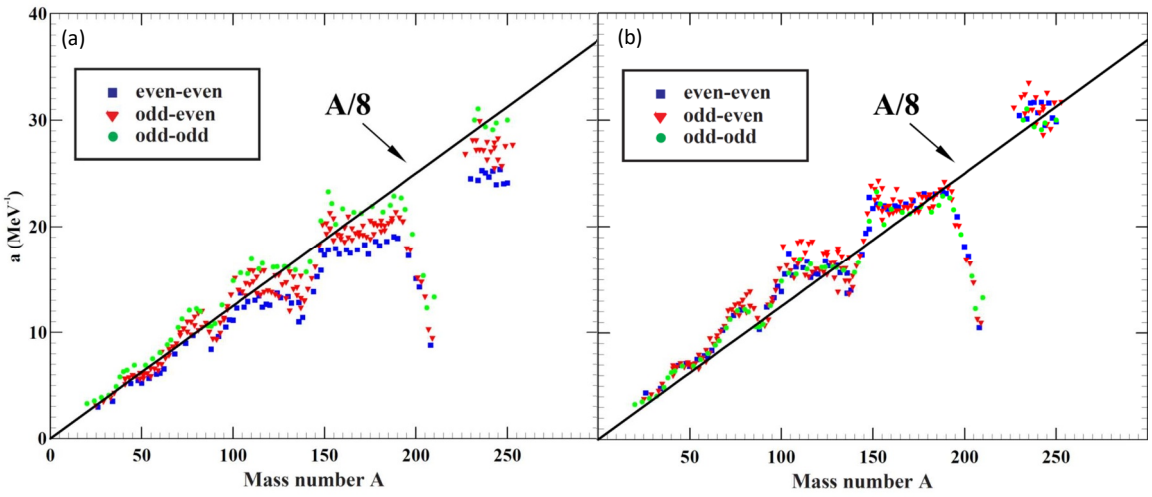

Figure 1. Level density parameter deduced from the s-wave neutron resonance mean spacing D_0 as function of the mass number. Panel (a) without pairing. Panel (b) with pairing (see text).

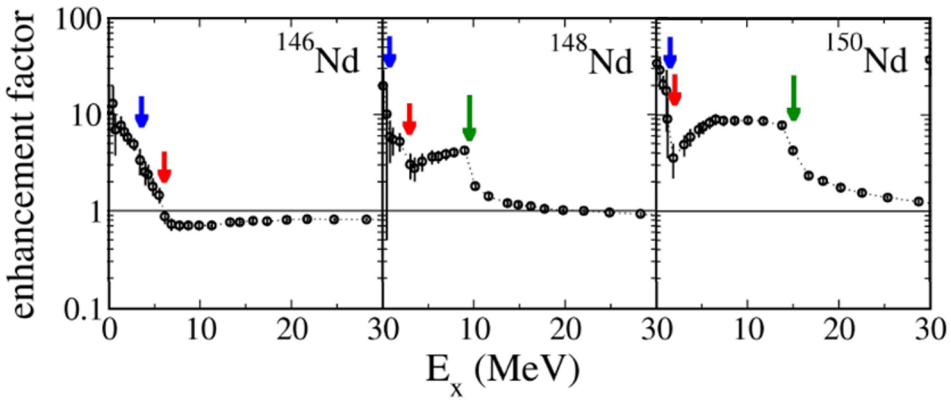

Figure 2. Enhancement factor in Nd isotopes as function of the excitation energy [11]. The blue and red arrows indicate where neutron and proton pairing, respectively, vanish. The green arrow indicates the excitation energy at which deformation starts to disappear.

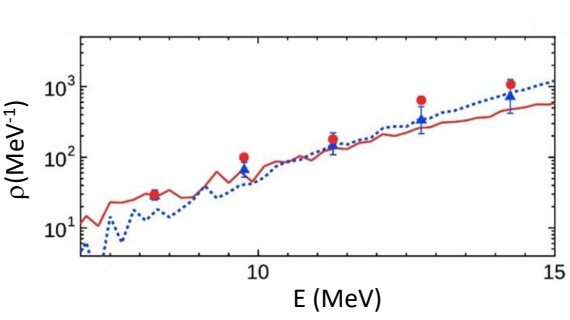

Figure 3. Level density of ^{58}Ni as a function of excitation energy. Theoretical results are shown by the red solid (J^π=2$^+$) and blue dotted (2$^-$) lines. Experimental data are given by circles (2$^+$) and triangles (2$^-$). Adapted from Ref. [13].

which proved its ability to reproduce experimental D_0's. It was then modified to improve the treatment of vibrational states [16] since feedback from fission cross section calculation showed that the adopted analytical enhancement was not appropriate [17]. Finally, the combinatorial approach was extended in 2012 [18] using the D1M Gogny interaction [19] within a temperature-dependent HFB calculation which enabled to describe consistently the damping of deformation, shell and pairing effects with increasing excitation energy. Last but not least, the quadrupole collective vibrational levels, also known as gamma and beta bands, which were previously determined by adjusting a phenomenological expression [15, 16] on experimental data, this time were predicted within the 5-dimensional collective Hamiltonian model [20]. Both combinatorial methods turned out to reach a level of accuracy on experimental resonance spacings similar to what is achieved by global analytical formulae, as can be observed in Fig. 4, but with the advantage of simultaneously providing a non-statistical low-energy spectroscopy. In both cases, tables have been produced and distributed [1, 21]. Improvements have also been recently and successfully achieved

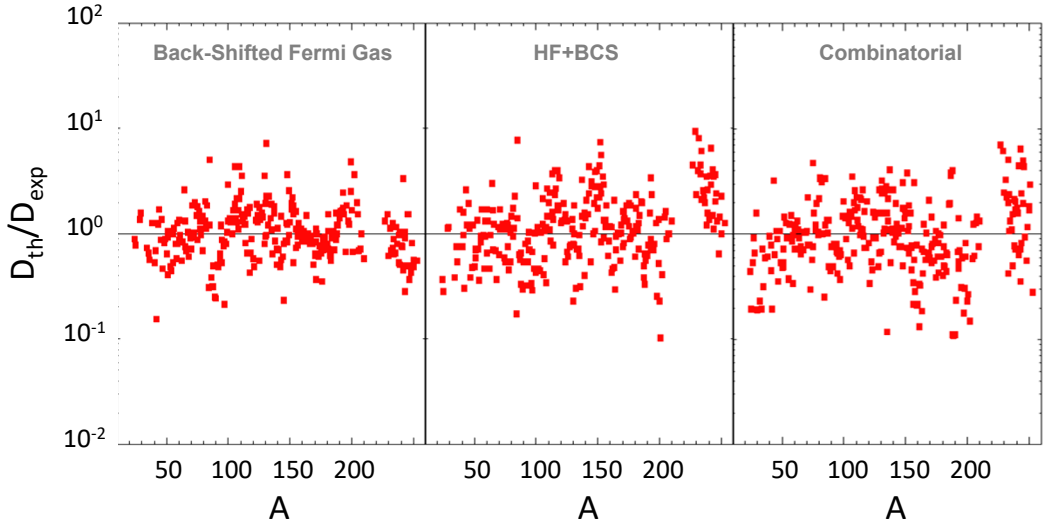

Figure 4. Ratio of the theoretical s-wave mean spacing D_{th} to the experimental D_{exp} as function of the mass number A for three theoretical approaches [21] (left panel), [14] (middle panel) and [16] (right panel), as described in the text.

in the description of NLDs for triaxial nuclei within the mean-field plus combinatorial approach on the basis of the BSkG3 interaction [22]. For such nuclei, the incoherent NLD is affected by the different single-particle level density at the triaxial deformation as well as the extra contribution stemming from the collective triaxial effects. Finally, let us mention that a recipe has also been proposed in Ref. [16] to offer the possibility to fit cross sections by shifting and renormalizing the tabulated level density as one traditionally does with the parameters entering the analytical phenomenological expressions.

4 The QRPA+Boson expansion approach

A new approach is now under development to go beyond the independent particle framework on which the previous statistical and combinatorial approaches rely [23]. The underlying idea is to take benefit from the success of QRPA approaches to describe low and high energy collective as well as non-collective states [24, 25] to get rid of the arbitrary separation of incoherent and coherent vibrational excited states.

More precisely, assuming an axially symmetric deformed nucleus, the QRPA approximation is employed to compute excited states stemming from quasiparticle excitations which induce a spin projection variation ΔK and parity π with respect to the ground state. In practice, the range for ΔK is between 0 and 9 for an even-even nucleus and between −9 and +9 for odd-A and odd-odd nuclei. Using the bosonic partition function as detailed in Ref. [26], it is then possible to compute within a combinatorial framework all multiphonon states, from which the level density can be directly deduced for an even-even nucleus. For odd-A and odd-odd nuclei, an extra step is required to couple the multiphonon states with all possible quasiparticles involving the blocked single nucleon(s) defining the nucleus ground state. For deformed nuclei, rotational bands are

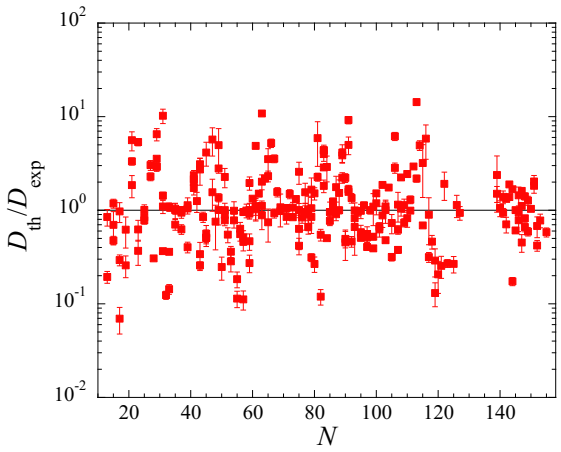

Figure 5. Ratio of the theoretical s-wave mean spacing D_{th} to the experimental D_{exp} as function of the mass number A obtained within the QRPA+Boson expansion method.

then constructed as in Ref. [26]. This new QRPA + Boson expansion (QRPA+BE) approach does not provide by default a good enough reproduction of s-wave mean spacings. However, QRPA predictions with the D1M interaction are known to overestimate the energies of the lowest collective levels by a few hundred keVs [24]. By applying a global shift to the QRPA energies [23], a rather good agreement is found with experimental s-wave mean spacings, as illustrated in Fig. 5.

These new level densities also compare fairly well with Oslo data and display a quite remarkable agreement with low energy spectroscopy. Typical examples are shown in Fig. 6. Among the differences with previous combinatorial approaches, one can note a rather narrower spin distribu-

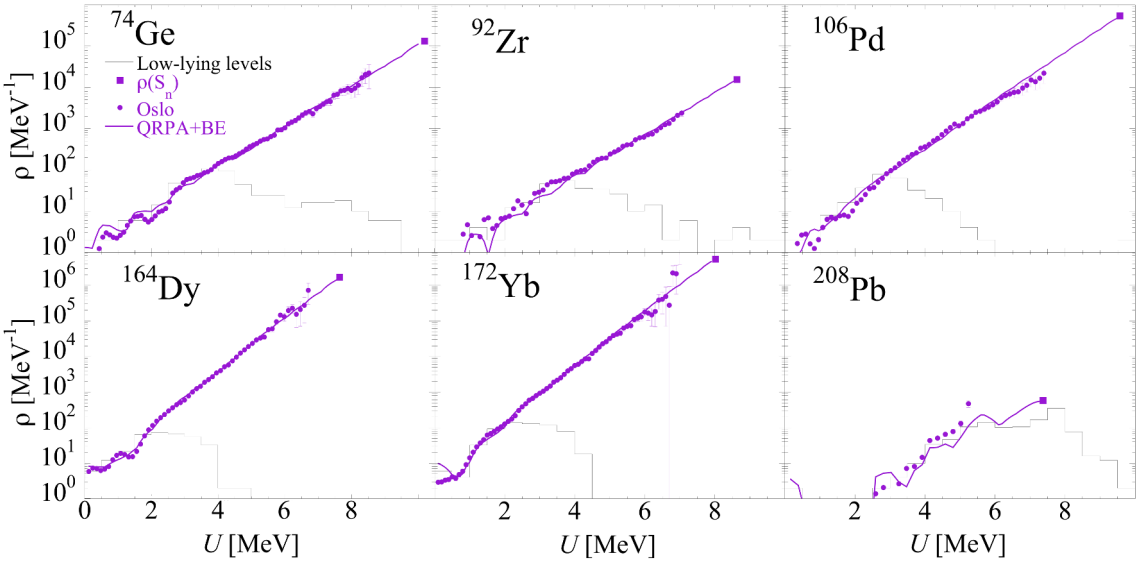

Figure 6. Theoretical and renormalized Oslo NLDs for 6 even-even nuclei between ^{74}Ge and ^{208}Pb. The black solid lines represent the NLD deduced from known discrete levels using an energy bin of 0.5 MeV. The solid circles correspond to the Oslo data [27] and the purple solid lines to the QRPA+BE predictions. The full squares at $U = S_n$ correspond to the total level density extracted from the QRPA+BE model after renormalization on experimental data following Ref. [28].

tion in comparison with more traditional models (see [23] for more details).

5 Conclusions and prospects

Despite 90 years of efforts, nuclear level densities are still the subject of intense work and the complicate intricacies of the various many-body effects that affect them still elude us. Several choices are available to compute them, from the simple phenomenological formulae to the most complex shell model based estimates, passing by the combinatorial approaches. When systematics are required as for astrophysical applications for instance, only mean-field-based statistical or combinatorial approaches can be used to compete with analytical expressions. They have now reached a rather good accuracy when compared with experimental data and the computational price to pay to produce tables, even if challenging for the most recent developments, is still achievable. The most sophisticated models remain computationally costly and cannot be used systematically. However, they can be precious to benchmark combinatorial approaches and control the underlying approximations on which they rely.

References

[1] R. Capote et al., RIPL – Reference Input Parameter Library for Calculation of Nuclear Reactions and Nuclear Data Evaluations, Nucl. Data Sheets **110**, 3107 (2009) and references therein, http://www-nds.iaea.org/RIPL-3. https://doi.org/10.1016/j.nds.2009.10.004

[2] H.A. Bethe, An Attempt to Calculate the Number of Energy Levels of a Heavy Nucleus, Phys. Rev. **50**, 332 (1936). https://doi.org/10.1103/PhysRev.50.332

[3] A. Gilbert and A. G. W. Cameron, A composite nuclear-level density formula with shell corrections, Can. J. Phys. **43**, 1446 (1965). https://doi.org/10.1139/p65-139

[4] G. Hansen and A.S. Jensen, Energy dependence of the rotational enhancement factor in the level density, Nucl. Phys. A **406**, 236 (1983). https://doi.org/10.1016/0375-9474(83)90459-1

[5] R. Sen'kov and V. Zelevinsky, Nuclear level density: Shell-model approach, Phys. Rev. C **93**, 064304 (2016). https://doi.org/10.1103/PhysRevC.93.064304

[6] W. E. Ormand and B. A. Brown, Microscopic calculations of nuclear level densities with the Lanczos method, Phys. Rev. C **102**, 014315 (2020). https://doi.org/10.1103/PhysRevC.102.014315

[7] G.H. Lang et al., Monte Carlo evaluation of path integrals for the nuclear shell model, Phys. Rev. C **48**, 1518 (1993). https://doi.org/10.1103/PhysRevC.48.1518

[8] S.E. Koonin et al., Shell model Monte Carlo methods, Phys. Rep. **278**, 2 (1997). https://doi.org/10.1016/S0370-1573(96)00017-8

[9] Y. Alhassid, Quantum Monte Carlo Methods for Nuclei at Finite Temperature, Int. J. Mod. Phys. B **15**, 1447 (2001). https://doi.org/10.1142/S0217979201005945

[10] Y. Alhassid, Auxiliary-field Quantum Monte Carlo Methods, Nuclei in Emergent Phenomena in Atomic Nuclei from Large-Scale Modeling: A Symmetry-Guided Perspective, ed. by K.D. Launey (World Scientific, Singapore, 2017), pp. 267–298. https://doi.org/10.1142/9789813146051_0009

[11] Y. Alhassid, private communication.

[12] C. Özen et al., Crossover from Vibrational to Rotational Collectivity in Heavy Nuclei in the Shell-Model Monte Carlo Approach, Phys. Rev. Lett. **110**,

042502 (2013). https://doi.org/10.1103/PhysRevLett.110.042502

[13] N. Shimizu et al., Stochastic estimation of nuclear level density in the nuclear shell model: An application to parity-dependent level density in ^{58}Ni, Phys. Lett. B **753**, 13 (2016). https://doi.org/10.1016/j.physletb.2015.12.005

[14] P. Demetriou and S. Goriely, Microscopic nuclear level densities for practical applications, Nuc. Phys. A **695**, 95 (2001). https://doi.org/10.1016/S0375-9474(01)01095-8

[15] S. Hilaire and S. Goriely, Global microscopic nuclear level densities within the HFB plus combinatorial method for practical applications, Nuc. Phys. A **779**, 63 (2006). https://doi.org/10.1016/j.nuclphysa.2006.08.014

[16] S. Goriely et al., Improved microscopic nuclear level densities within the Hartree-Fock-Bogoliubov plus combinatorial method, Phys. Rev. C **78**, 064307 (2008). https://doi.org/10.1103/PhysRevC.78.064307

[17] M. Sin et al., Neutron-induced fission cross section on actinides using microscopic fission energy surfaces, Proceedings of the International Conference on Nuclear Data for Science and Technology, 22–27 April 2007, Nice, France, edited by F. Gunsing, E. Bauge, R. Jacqmin, S. Leray, and O. Bersillon (EDP Sciences, Les Ulis, France, 2008), p. 313, https://doi.org/10.1051/ndata:07370

[18] S. Hilaire et al., Temperature-dependent combinatorial level densities with the D1M Gogny force, Phys. Rev. C **86**, 064317 (2010). https://doi.org/10.1103/PhysRevC.86.064317

[19] S. Goriely et al., First Gogny-Hartree-Fock-Bogoliubov Nuclear Mass Model, Phys. Rev. Lett. **102**, 242501, (2009). https://doi.org/10.1103/PhysRevLett.102.242501

[20] J.-P. Delaroche et al., Structure of even-even nuclei using a mapped collective Hamiltonian and the D1S Gogny interaction, Phys. Rev. C **81**, 014303 (2010). https://doi.org/10.1103/PhysRevC.81.014303

[21] A. J. Koning et al., TALYS: modeling of nuclear reactions, Eur. Phys. J. A **59**, 131 (2023). https://doi.org/10.1140/epja/s10050-023-01034-3

[22] S. Goriely et al., Improved microscopic nuclear level densities within the triaxial HFB plus combinatorial method, Phys. Rev. C (2025) to be submitted

[23] S. Hilaire et al., A new approach to nuclear level densities: The QRPA plus boson expansion, Phys. Lett. B **843**, 137989, (2023). https://doi.org/10.1016/j.physletb.2023.137989

[24] S. Goriely et al., The Gogny-HFB+QRPA dipole strength function and its application to radiative neutron capture cross section, EPJ Web of Conferences **178**, 04001 (2018). https://doi.org/10.1051/epjconf/201817804001

[25] S. Goriely et al., Reference database for photon strength functions, Eur. Phys. J. A **55**, 172 (2019). https://doi.org/10.1140/epja/i2019-12840-1

[26] S. Hilaire et al., Combinatorial nuclear level densities based on the Gogny nucleon-nucleon effective interaction, Eur. Phys. J. A **12**, 169 (2001). https://doi.org/10.1007/s100500170025

[27] Oslo database : Level densities and gamma-ray strength functions, https://www.mn.uio.no/fysikk/english/research/about/infrastructure/ocl/nuclear-physics-research/compilation/

[28] S. Goriely et al., Comprehensive test of nuclear level density models, Phys. Rev. C **106**, 044315 (2022). https://doi.org/10.1103/PhysRevC.106.044315